MANAGEMENT OF SOIL EROSION AND SEDIMENT YIELD IN SEMI-ARID REGIONS, A CASE STUDY OF WADI SUDR WATERSHED, SOUTH SINAI, EGYPT

Ismail FATHY[1], Hend ADEL[1,*], Elsayed M. RAMADAN[1], Ahmed HELMY[1], Hany F. ABD-ELHAMID[1,2], Ahmed M. NOSAIR[3]

[1] *Water and Water Structures Engineering Department, Faculty of Engineering, Zagazig University, Zagazig 44519, Egypt, smokhtar@zu.edu.eg, hany_farhat2003@yaho.com, h.ali021@eng.zu.edu.eg, ahelmy2010@hotmail.com, ismailfathy1982@gmail.com*

[2] *Department of Environmental Engineering, Faculty of Civil Engineering, Technical University of Košice, 042 00Košice, Slovakia, hany.abdelhamid@tuke.sk*

[3] *Environmental Geophysics Lab. (ZEGL), Geology Department, Faculty of Science, Zagazig University, Zagazig 44519, Egypt; ahmed_nosair@zu.edu.eg*

**Corresponding author: h.ali021@eng.zu.edu.eg*

Abstract: Controlling soil erosion and sediment yield is crucial for conserving soil and water resources. Although extensive research has examined this issue globally, the specific impacts of management practices on Wadi Sudr watershed have not yet been studied. This study aims to evaluate the impacts of mulching and check dam scenarios on sediment yield and soil erosion in Wadi Sudr, employing multi-regression analysis to forecast the percentage reductions achieved through these management practices. The Sediment Delivery Ratio (SDR) and Revised Universal Soil Loss Equation (RUSLE) models were integrated within ArcGIS to analyze sediment yield and soil erosion, examining the consequences of various recurrence intervals. Soil erosion was classified into five categories, ranging from severe to low. The most dominant category in Wadi Sudr is very low, covering 75% of the total area. The Al-Athamy sub-basin exhibited the highest soil erosion (17 t/ha/yr) and sediment yield (5.23 t/ha/yr) at the 100-year recurrence interval, prompting the implementation of management practices. Mulching with length ratios of 11,680 m, 25,980 m, and 32,320 m reduced soil erosion by 3%, 7%, and 9% and sediment yield by 19%, 23%, and 24%, respectively. Check dams though effective in reducing sediment yield by 35% and 86% for dams 1 and 2, minimally impacted soil erosion and were unsustainable and expensive. Results highlight mulching as the most cost-effective and sustainable management practice. These findings provide valuable insights for policymakers in developing effective soil and water conservation strategies to safeguard semi-arid watersheds.

Keywords: Soil erosion, Sediment yield, RUSLE, SDR, Mulching, Check dams.

1. INTRODUCTION

Globally, the most severe type of land degradation is soil erosion, leading to approximately 85% of land degradation worldwide (Phinzi and Ngetar, 2019). A variety of erosive parameters, such as wind, rain, ice, and runoff, can cause soil erosion, which results in the separation of soil particles and the loss of productive land. Additionally, it causes the deterioration of water quality and a reduction in reservoir capacity (El Jazouli et al., 2017). Africa, South America, and Asia have the highest annual average soil erosion rates, ranging between 30 and 40 tons/ha (Pimentel, 2006). The main causes of soil erosion hazards include population growth, deforestation, unsustainable agricultural practices, removal of natural vegetation, misuse of soil and water resources, poor farming methods, burning of biomass, and overgrazing (FAO, 1990). In arid areas, the primary factor responsible for erosion and sediment yield is water flow (Alhamid and Reid, 2002). Due to the lack of vegetation and poor soil surface infiltration capacity, arid regions are highly vulnerable to flash floods during rainfall events. This may lead to massive volumes of surface runoff, leading to soil erosion and sediment yield (Al-Bassam et al., 2014). Sediment yield is the amount of sediment that has accumulated at the basin outlet. Thus, identifying hotspot areas that need effective soil conservation measures and precisely measuring the amount of soil erosion is essential for a soil conservation plan's efficacy.

Various models are used globally to calculate spatio-temporal sediment yield and soil erosion. These models include physically-based models such as ANSWERS (Beasley et al., 1980), WEPP (A. Nearing et al., 1989), EUROSEM (Morgan et al., 1998), (SEMMED) (De Jong et al., 1999), and (SWAT) (Arnold and Fohrer, 2005). Empirical models such as (RUSLE) (Renard et al., 1997), (MUSLE) (Williams, 1975), and (USLE) (Wischmeier and Smith, 1978b). The Sediment Delivery Ratio (SDR) was used to estimate the sediment yield (Saoud and Meddi, 2023). The most widely used empirical model for soil erosion estimation is RUSLE because it requires limited data, is simple to implement, and is suitable for geospatial platforms (Millward and Mersey, 1999). However, it is not capable of estimating sediment yield. The five factors contributing to estimate soil erosion using the RUSLE model are the topographic factor (LS factor), cover management factor (C factor), rainfall erosivity factor (R factor), soil erodibility factor (K factor), and management practice factor (P factor). GIS can effectively manage spatial data by interpolating, processing, and mapping the overlaying and spatial characteristics of rainfall, vegetation cover, topography, the watershed's soil, and land use (Elewa et al., 2020).

Soil loss and sediment yield were estimated by combining the RUSLE and SDR models (Rajbanshi and Bhattacharya, 2020). (Mhaske et al., 2021) merged the RUSLE model with the Analytic Hierarchy Process (AHP) in India with the objective of evaluating soil erosion and identifying regions that are most suitable for sediment deposition. (Assis et al., 2021) estimated the soil erosion and sediment yield using the USLE model and a DH-48 sampler in Brazil. (Aslam et al., 2021) utilized the RUSLE model in Pakistan for future climatic and land cover scenarios for 2030 and 2040, assessing soil erosion annually based on sediment yield trends and geographical dispersion. In addition to Markov chain analysis, artificial neural networks (ANN) were utilized to model future land cover changes. (Abebe et al., 2023) examined sediment connectivity and assessed sediment yield in Southeast Spain by integrating the Sediment Delivery Ratio (SDR), Index of Connectivity (IC), and RUSLE model. (Salhi et al., 2023) estimated soil erosion by integrating morphometric analysis, field monitoring, and the RUSLE model in Morocco. RUSLE has been used by many researchers to estimate soil erosion in Egypt (Darwish et al., 2015). Additionally, (Kawy and El-Nady, 2012) estimated soil erosion by using both USLE and RUSLE in the Eastern Desert of Egypt. (Selmy et al., 2021) integrated USLE and ILSWE to estimate water and wind erosion in Dakhla Oasis, Egypt. (Abd-Elaty et al., 2022) suggests examining how sediment yield in the Sinai Peninsula is affected by varying recurrence intervals.

There are numerous methods for preventing soil erosion, such as contour planting, mulching, soil netting, and building physical structures like check dams. Other methods include using biopolymers, geotextile materials, plastics, rubber mulch, chemical treatments as soil binders, and modified weed control (Kumarasinghe, 2021). A variety of engineering and biotechnological techniques, including afforestation, grass planting, construction of check dams, terracing, creating reservoirs, filling gullies, and establishing cropland, are used to reduce soil loss and conserve water (Dong et al., 2022).

Check dams are an efficient conservation method used worldwide for conserving water and soil (Abbasi et al., 2019). They offer several benefits: they slow down intense flow rates, prolong the lag time, trap sediments, increase vegetation, improve the permeability of the channel, and lower flood peak discharge in the watersheds (Abbasi et al., 2019). Mulching is a cost-effective soil erosion control method in which organic and inorganic materials are applied to the topsoil to prevent erosion (Kumarasinghe, 2021). Several researchers have assessed the ability of Management Practices to reduce soil erosion and sediment load,

The SWAT model was applied by (Shi et al., 2019) to investigate how sediment yield is impacted by check dams and changes in land use. (Zhao et al., 2017) used fieldwork and the SEDD model how check dams and changes in land use in the Loess Plateau, China, impact sediment yield. (Boix-Fayos et al., 2008)) examined the reduction in sediment yield after implementing changes in land use and constructing check dams based on the WATEM-SEDEM model and fieldwork in Spain. The combination of soil/stone bunds and grassed waterways was the most effective management scenario based on the SWAT model when waterways, filter strips, soil/stone bunds, and cropland reforestation were applied in Ethiopia (Gashaw et al., 2021). In Nigeria, (Adekalu et al., 2007) evaluated the impact of elephant grass mulch on soil loss. (Bombino et al., 2021) found that Mulching with residues was the most effective BMP compared to mechanical tillage and standard protection in Southern Calabria, Italy. Soil/stone bunds and terracing were the most effective management practices using the SWAT model in Ethiopia (Leta et al., 2023).

Wadi Sudr is one of Sinai's most significant watersheds. It has experienced numerous flash floods over the last few decades and has suffered from soil erosion and sediment yield issues. These flash floods cause severe damage to dissecting roads, infrastructures, and farms in the vicinity of the watershed and the tourist area at Ras Sudr City located in the coastal zone of the Wadi delta. There are some studies conducted in Wadi Sudr as follows: Remote sensing and fieldwork approaches were integrated to evaluate the hydrological characteristics of the wadis impacting Ras Sudr (Gabr and El Bastawesy, 2015). The risk of flooding was evaluated in Wadi Sudr by combining GIS, remote sensing, hydrodynamic, and hydrologic modeling (Ali, 2023). The geomorphological characteristics of Wadi Sudr were analyzed to determine the threat of flash floods and offer appropriate mitigation techniques (Ramadan et al., 2022). The disturbed model is the best runoff hydrograph simulator when compared with lumped and semi-disturbed in Wadi Sudr (Fathy et al., 2015).

According to literature reviews, several studies have focused on soil erosion and sediment yield modeling in other regions of the world, but no prior studies have addressed these issues in Wadi Sudr. This paper aims to fill that gap by studying soil erosion and sediment yield in Wadi Sudr, as well as proposing measures to control them and forecasting their reduction after applying best management practices (BMPs). The main objectives of this research are (a) Forecast sediment yield and soil erosion related to rainfall events based on different recurrence intervals, (b) Integrate the SDR model and RUSLE model to evaluate sediment yield and soil erosion, (c) assess different management scenarios, such as mulching and checking dams in the highest sediment yield and soil erosion subbasins, (d) Examine the best management scenarios and evaluate the effects of these scenarios on sediment yield and soil erosion reduction, (e) Forecast the soil erosion and sediment yield reduction percentage by developing empirical equations considering the application of the BMP, (f) Identify the methodology of sediment yield, soil erosion, and sediment control calculation to help policymakers take appropriate actions in any study area. Finally, this research will assist policymakers in implementing appropriate management practices to prevent soil erosion, control sediment yield, and consequently protect lives and property.

2. MATERIALS AND METHODS

2.1. Description of the study area

Wadi Sudr is in southwestern Sinai, Egypt, spanning between latitudes 29˚37'33" to 29˚58'44" N and longitudes 32˚42'29" to 32˚18'28" E (Figure 1a). The watershed flows westward and discharges water into Suez Gulf. It covers approximately 600 km2 and is classified into 19 sub-watersheds (Figure 2a). Ras Sudr area includes recreational activities, tourist hubs, urban zones, oil infrastructure such as tanks and pipelines, as well as cultivated land.

2.2. Climate

The climate of Sinai Peninsula is highly arid, with prolonged, dry, and hot summers, along with mild winters. Occasionally, certain areas of Sinai experience intense rainfall during winter, leading to flash floods. The average temperature exceeds 36°C in the summer and is around 8°C in the winter and the mean annual rainfall ranges from 9.33 to 39.9 mm (see Figure 2b) (Soliman et al., 2017).

2.3. Geologic settings

Geologically, Wadi Sudr consists of rocks from the Upper Cretaceous to the Quaternary age (Hasanein, 1989), (Figure 1b).

Upper Cretaceous: Differentiated into Matallah and Sudr Formations, occupying mainly the eastern parts of the watershed. The Matallah Formation consists of sandy shale with intercalations of limestone and phosphatic marl, with a thickness varying between 65 and 165 meters.

Tertiary rocks are classified into the Esna Formation, the Ras Malab Evaporite Group, and the Gharandal Group (Figure 1b). The Esna Formation belongs to the Paleocene age, with a thickness of 40 meters, and is composed of grayish-yellow marly material with a dark green shale limestone band in the center. The Thebes Formation, dating back to the Eocene age, primarily consists of chalky limestone. At its base, it contains flint bands and nodules, while thin successive chert bands appear at the top. The Ras Malab Evaporite Group is located downstream of Wadi Sudr. The Gharandal Group consists of the Uyun Musa and Sumar Formations.

Quaternary deposits are composed of wadi, sabkha, and undifferentiated Quaternary deposits, which are commonly found in the downstream areas of Wadi Sudr (Figure 1b).

2.4. Data Processing

Soil erosion evaluation relied on analyzing the study area characteristics, including topography, soil type, land use/land cover, and climate. During the mapping process for these characteristics, the data utilized were gathered from diverse sources. For Wadi

Sudr, a Digital Elevation Model (DEM) with a resolution of 30 m was acquired from Earth Explorer (https://earthexplorer.usgs.gov/). Topographic parameters, including slope and hydrographic

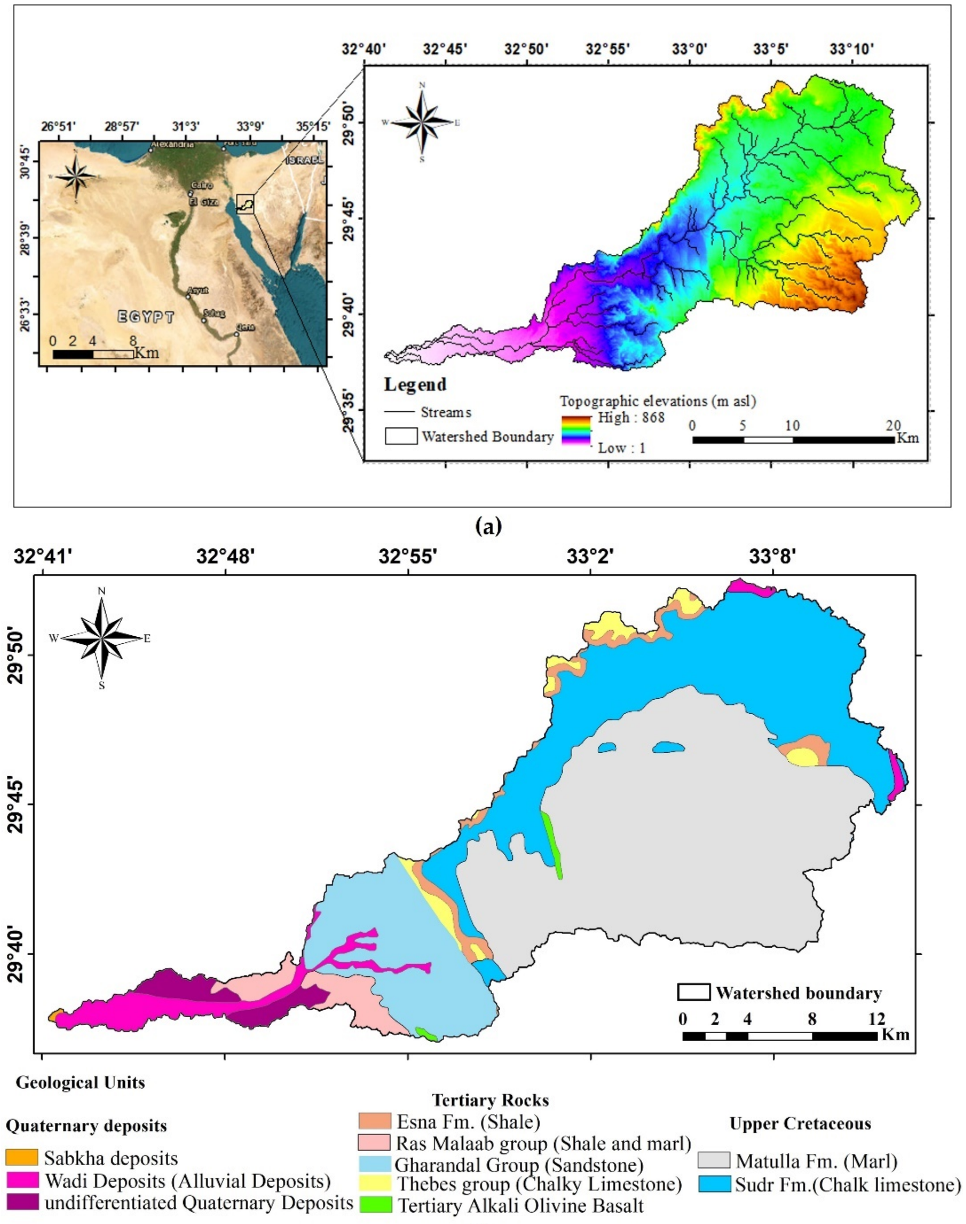

Figure 1. (a) The location map, (b) Geological map (Scale 1:250,000) (CONOCO, 1987).

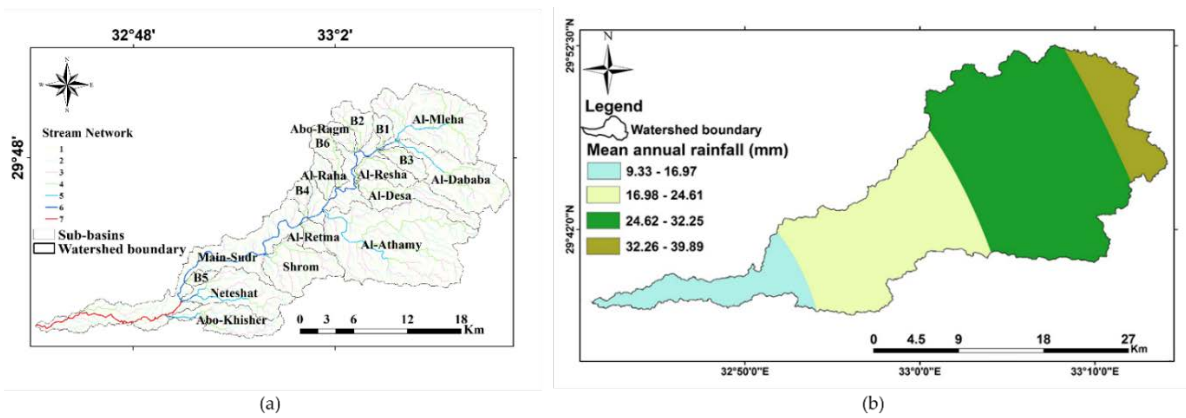

Figure 2. Wadi Sudr characteristics (a) Sub basins, and (b) The mean annual rainfall.

network, were generated from this data. Average annual rainfall data for 21 years (from 2000 to 2020) were obtained from eight rainfall stations within Sinai region, obtained from the Meteomanz site (http://www.meteomanz.com/?l=1). The map of the soil was accessed from the Food and Agriculture Organization Digital Soil Map of the World (FAO DSMW)(https://data.apps.fao.org/map/catalog/static/search? keyword=DSMW). Esri Land Use/Land Cover data were utilized to generate LU/LC maps (https://livingatlas.arcgis.com/landcover/).

2.5. Methodology

Figure 3 shows the flow chart of the methodology used in the current study. In this methodology, RUSLE-SDR models are used to evaluate soil erosion and sediment yield in Wadi Sudr and to predict these by analyzing the impact of different recurrence intervals. In addition, management practices are proposed for hotspot areas to control soil erosion and sediment yield. The soil erosion and sediment yield reduction are forecasted using a regression model.

2.6. RUSLE model

Soil erosion was assessed in this research by applying RUSLE to spatially depict erosion sensitivity in Wadi Sudr watershed. RUSLE was integrated with GIS to analyze the erosion process. ArcGIS software was used to estimate and map the erosion factors. Ultimately, the implementation of RUSLE facilitated the evaluation of water erosion and its contributing parameters, as well as the forecasting of soil erosion based on rainfall events at various

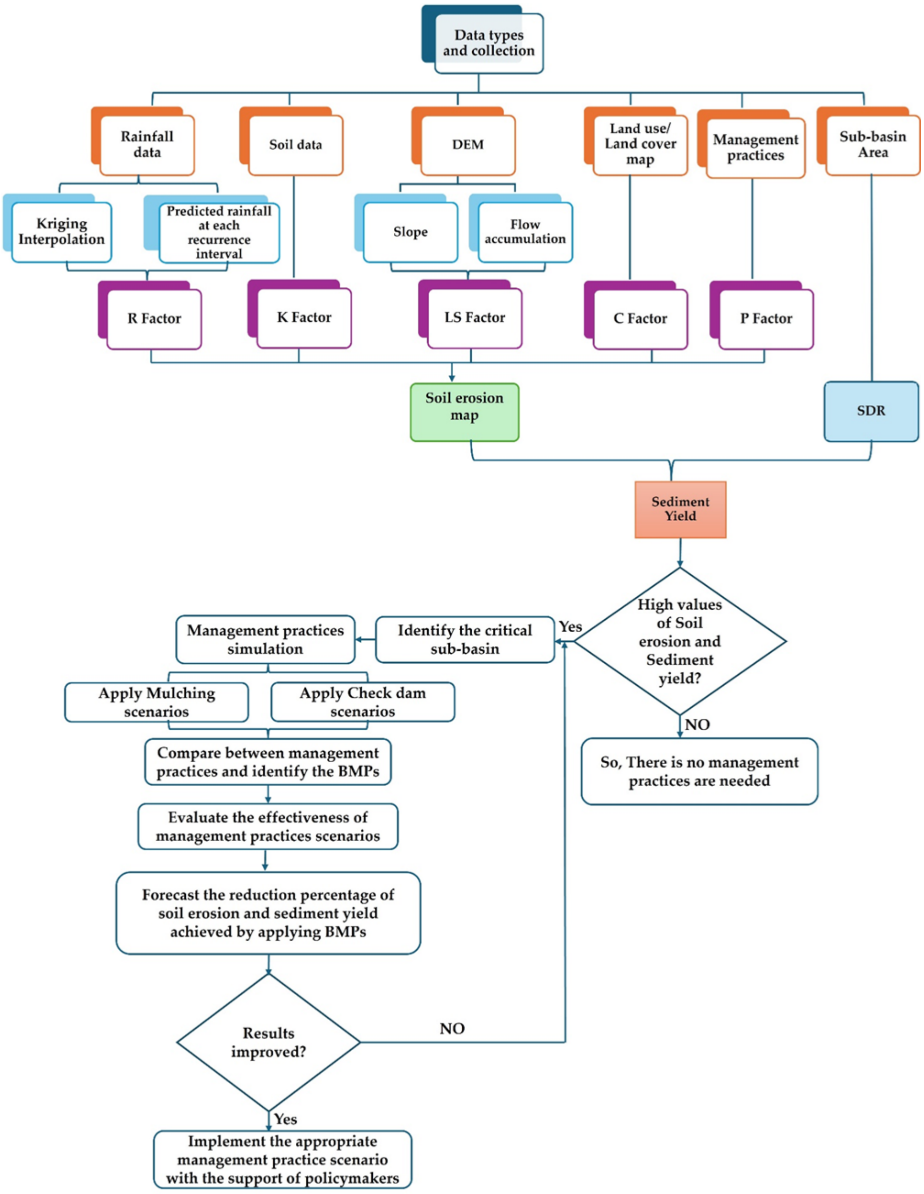

Figure 3. Flow chart of the methodology applied in the current study.

recurrence intervals. RUSLE is numerically represented by Eq. 1 (Renard, 1997).

$$A = R \times LS \times K \times P \times C \quad (1)$$

where,

A represents the mean soil loss per year (ton/ha/yr), R is the rainfall-runoff erosivity index (MJ mm/ha/hr/yr), LS corresponds to the topography (dimensionless), K represents the erodibility of soil (t /ha/ MJ mm/ha/hr/yr), P is the support practice index (dimensionless), and C represents the cover management (dimensionless).

2.6.1 Rainfall Erosivity (R-factor)

The R factor measures the impact of raindrops on the soil, as well as the rate and quantity of runoff, which is the primary mechanism responsible for sediment yield and accounts for 80% of soil loss (Zerihun et al., 2018). Eq. 2, is used to evaluate the R-factor (Choudhury and Nayak, 2003).

$$R = 79 + 0.363X \quad (2)$$

where,

R is the annual rainfall-runoff erosivity index,

X is the average yearly rainfall (mm).

Table 1. Coordinates of the stations

Station	X	Y	Z
Al-Arish Intl	33.8	31.1	36.9
El Tor	33.7	28.2	35.0
Hurghada	33.8	27.2	14.0
Nekhel	33.7	29.9	403.0
Port Said Elgamil	32.2	31.3	6.0
Ras Sedr	32.7	29.6	16.0
St Catrine	34.1	28.7	1331.0
Abu-Rudees	33.1	28.5	7.0

Rainfall data for 21 years (2000-2020) were collected from eight stations located within or near the watershed (Al-Arish, El-Tor, Hurghada, Nekhel, Port Said Elgamil, Ras Sudr, Saint Catherine, and Abu Rudees) (Table 1). The average annual precipitation for the watershed was assessed based on its spatial distribution using the kriging interpolation method in ArcGIS. Predicted rainfall depths at recurrence intervals of 2, 5, 10, 25, 50, and 100 years were derived using Hyfran Plus software based on the hydrological frequency analysis tool, considering different distributions such as GEV, exponential, Weibull, Gamma, Gumbel, Log-Pearson Type III, and Normal. Using the exponential distribution and best-fitting analysis, the most appropriate distribution was identified. Subsequently, the predicted rainfall obtained from Hyfran Plus software was used to estimate the R factor at different recurrence intervals.

2.6.2 Soil Erodibility (K-Factor)

The K factor evaluates the vulnerability of soil particles to detachment and yield caused by runoff (Wischmeier and Smith, 1978b). It is affected by the soil's structure, permeability, and organic matter content, as well as the proportions of clay, sand, and silt present (Erencin et al., 2000). The K factor ranges from zero to one, with lower values indicating soils that are less vulnerable to erosion, while soils susceptible to severe erosion have greater values of the K factor (Pancholi et al., 2015). The FAO Digital Soil Map of the World (DSMW) was used to produce soil maps. Within ArcGIS, the layer of soil data was trimmed to Wadi Sudr. Equation 3, along with the parameters outlined in Equations 4 to 7, was utilized to evaluate the K-factor.

$$K = \mathrm{Fhisand} \times \mathrm{Forgc} \times \mathrm{Fsi-cl} \times \mathrm{Fcsand} \times 0.1317 \quad (3)$$

$$\mathrm{Fhisand} = \left(1 - \frac{0.7 \times SN1}{SN1 + e^{(-5.51 + 22.9 \times SN1)}}\right), \quad (4)$$

$$\mathrm{Forg} = \frac{(1 - (0.256 \times C))}{(C + e^{3.72 - 2.95 \times C})}, \quad (5)$$

$$Fsi - cl = \left(\frac{SIL}{CLA + SIL}\right)^{0.3}, \text{ and} \quad (6)$$

$$\mathrm{Fcsand} = 0.2 + e^{\left(-0.0256 \times SAN \times \left(\frac{1 - SIL}{100}\right)\right)}. \quad (7)$$

where,

SIL represents % silt,

SAN represents the sand percentage,

C is the organic carbon content,

CLA corresponds to the %clay, and

$SN1 = \frac{SAN-1}{100}$,

Fcsand is the low index of soil erodibility.

Fsi-cl is the high clay-to-silt ratio and low K-factor.

Forg represents a factor in soil that is rich in organic matter that reduces soil erodibility.

Fhisand reduces the erodibility of soil with a high sand content.

2.6.3 Land use Management (C-Factor)

The most significant factor in soil erosion studies is its ability to control soil erosion. It ranges from 0 to 1, with a C value of 1 signifying a desolate area without cover. However, a C value below 1 denotes the presence of cover that can protect the soil from erosion (Pham et al., 2018). The C factor was estimated using the Sentinel-2, 10-meter LU/LC time series of Esri Land Cover through an unsupervised classification method in the GIS software. LU/LC raster map was transformed into a vector format file. Subsequently, Each land-use class is associated with a

C-factor value, including bare land, rangeland, urban, and cropland (Table 4). (Venter et al., 2022) revealed that, in comparison to ESA's World Cover (WC) and Google's Dynamic World (DW), Esri is the most accurate approach

2.6.4 The Topographic index (LS-Factor)

It illustrates how slope steepness and length affect water-induced erosion, including rill, inter-rill, and sheet erosion. It integrates slope steepness (S) and slope length (L), indicating how far the runoff starts to concentrate from the upper boundary of the parcel (Khairunnisa et al., 2020). Significant erosion is commonly caused in steeply sloped areas. GIS software generated the LS map through the following steps: filling the DEM, then generating the slope map, flow accumulation (Fa), and flow direction. Afterward, the LS factor was estimated using Eq. 8 in a raster calculator.

$$LS = (Fa \times \left(\frac{\text{cell size}}{22.13}\right))^{0.4} \times (Sin\left(\frac{\text{slope}\times 0.01745}{0.09}\right))^{1.4} \times 1.6 \quad (8)$$

2.6.5 Management Practices (P-Factor)

It is generally determined by practices that reduce the effects of various contributing variables on soil erosion. In this study, the management practice index is 1, as no conservation measures were implemented, resulting in the highest expected erosion under baseline conditions. However, after applying mulching and checking dam scenarios, the P factor will take on different values.

2.7 SDR model

By integrating the RUSLE/SDR method, the Sediment yield (SY) (ton/ha/year) for each sub-basin was estimated within ArcGIS. SY represents the sediment discharge at specific points over a designated interval from each sub-basin (Thomas et al., 2018). SDR refers to the proportion of transported sediment in the river system to a specific location compared with the soil loss (ton/ha/yr) upstream of that location (Silva et al., 2013). Sediment yield represents eroded soil amount from the watershed transported by flow, with the highest amounts of SY found in areas with steep slopes, scrublands, and sandy soils. (SDR) estimates the overall sediment volume transported out of the watershed (Gelagay and Minale, 2016). SDR and annual average potential soil erosion (A) were integrated for sediment yield estimation Wadi Sudr watershed, The Soil Conservation Service of the United States Department of Agriculture (USDA, 1972) has endorsed the SDR as shown in Equation 9.

$$SDR = 0.51A^{-0.11} \quad (9)$$

where A is the watershed area in kilometer square. The sediment yield in each catchment was computed by applying Equation 10, which incorporates SDR values with annual average soil loss, utilizing the statistical methodology outlined by (Wischmeier and Smith, 1978a):

$$SY = SDR \times A \quad (10)$$

3. RESULTS AND DISCUSSION

Sediment yield, soil erosion, and their contributing factors were spatially estimated in Wadi Sudr watershed, and management practices were proposed in the Al-Athamy sub-basin. In addition to forecasting soil erosion and sediment yield reduction percentage based on the BMP. The results are discussed in the following subsections.

3.1. RUSLE model results

3.1.1. LS-factor results

It illustrates how soil erosion is affected by topography, calculated from the DEM and is dependent on slope steepness and length. It ranges from 0 to 48 (see Figure 4d). In mountainous and steeply sloped areas with slopes greater than 25º (see Figure 4c) the highest LS values were found. These zones have a high potential for runoff, as indicated in the slope map. As the LS factor increases, soil erosion also increases.

3.1.2. Soil Erodibility results

The K-factor is regarded as the primary challenge in soil erosion modeling because of the inadequate availability of data regarding soil attributes. For almost the entire basin, the K-factor is associated with Eutric Regosols. Only at the basin's outlet are Calcic Yermosols present, indicating moderate soil erodibility (Table 2, and Figure 4a).

Table 2. K factor values for various topsoil surfaces in Wadi Sudr watershed.

FAO soil sample	Topsoil sand	Topsoil silt	Topsoil clay	Topsoil organic carbon	f_{csand}	$f_{cl\text{-}silt}$	f_{orgc}	f_{hisand}	K_{RUSLE}
Calcic Yermosols	68.3	15.1	16.6	0.5	0.26	0.8005	0.98	0.963	0.02687
Eutric Regosols	63.5	17.9	18.7	0.26	0.278	0.8068	0.99	0.985	0.02912

Table 3. Predicted rainfall depths at different recurrence intervals and Rainfall erosivity factor.

Years	Predicted Rainfall depth (mm)	R-Factor (MJ mm /ha/h/yr)
2	27.2	88.8736
5	40.5	93.7015
10	49.4	96.9322
25	60.5	100.9615
50	68.8	103.9744
100	77	106.951

3.1.3. R-Factor results

Erosivity denotes the vulnerability of soil erosion. The mean annual rainfall recorded at eight rainfall stations, produced by kriging interpolation in ArcGIS, ranges from 9.33 to 39.89 mm. The highest annual mean rainfall rates are found in zones with high altitudes, while areas with lower rainfall values exist in low-altitude zones within the Wadi (Figure 2b). The predicted rainfall depths determined by Hyfran Plus software for various recurrence intervals follow a similar trend as the R factor (Table 3). It was evident that soil erosion increases with rising R-factor values, particularly under scenarios of more frequent and intense rainfall events.

3.1.4 C-factor results

It is regarded as a reduction management tool, reflects land use changes in the Wadi, and is associated with a value for each land use type, for bare ground (1), rangeland (0.7), crops (0.28), and built-up areas (0) (Table 4). The smallest values are found at the outlet of the wadi in the western-southern part, ranging from 0.0 to 0.28, resulting in the lowest soil erosion rates due to the existence of crops and built-up areas, which decrease soil erosion. Most of the wadi have higher values of C-factor, spanning between 0.7 and 1, which is attributed to bare ground and rangeland, leading to increased soil erosion (Figure 4b). In general, as vegetation increases, the soil erosion rate decreases, thereby reducing runoff velocity.

Table 4. The values C-Factor in Wadi Sudr watershed (Maqsoom et al., 2020).

LU/LC types	C-Factor	% Area
Bare ground	1	76%
Rangeland	0.7	23.5%
Crops	0.28	0.3%
Built-up areas	0	0.2%

3.1.5. Soil Loss (A) results

To estimate the soil loss, RUSLE was integrated with GIS. The topographic factor, rainfall erosivity factor, cover management factor, soil erodibility factor, and management practice factor all contribute to estimating it. Predictions of soil loss were made corresponding to different recurrence intervals. The findings from modeling these variables are depicted in Figure 5. The R-factor is very effective in soil erosion estimation, as potential soil erosion increases with recurrence intervals due to increased rainfall. LS factor and C factor are the dominant factors influencing soil erosion. The LS factor increases in steep slope areas, leading to higher potential runoff and causing greater soil loss. The C factor decreases in areas with vegetation cover, which reduces the impact of erosion, in bare areas, which are highly susceptible to erosion. Zones with a high soil erodibility factor are exposed to higher rates of soil erosion, while zones with lower soil erodibility values have lower erosion rates due to the soil in these regions resisting erosion.

The potential soil erosion in ton/ha/year in Wadi Sudr was categorized into five classes for visual interpretation: severe (>33.6), high (22.4 to 33.6), moderate (11.2 to 22.4), low (6.7 to 11.2), and very low (<6.7) (Selmy et al., 2021). Most of the Wadi falls under the very low class (73%), with 13% in the low category (the very low and low class occurred in areas with gentle slopes where the land lay nearly flat), 10% in the moderate class (which occurs in moderately sloped areas), and 2% of the Wadi in the severe and high classes which found in steeply sloped regions, particularly those left bare and unprotected, where the lack of vegetation allowed erosion to gain a relentless foothold (Figure 5).

The average annual soil loss (Am) increases with recurrence intervals as the rainfall erosivity factor follows the same trend as rainfall by a 5% increase percentage in each recurrence interval (Table 5). The Am has a range from (0 to 106), (0 to 112), (0 to 116), (0 to 121), (0 to 124), and (0 to 128) ton/ha/year at return periods (TR) of 2, 5, 10, 25, 50,100 years respectively (Figure 6). The zones with the highest soil loss rates were bare lands with no conservation practices, steeply sloped highlands, tributaries, and streamlines that carry high sediment loads. The lowest soil loss values were found in plain areas and agricultural land.

Table 5. Average soil loss at different recurrence intervals (TR).

Recurrence interval (TR)	2	5	10	25	50	100
Average soil loss (ton/ha/year)	6.2	6.55	6.74	7.03	7.24	7.44

3.2. SDR model results

The RUSLE-SDR models were integrated for sediment yield estimation. SDR in the Wadi Sudr watershed was determined using the theoretical

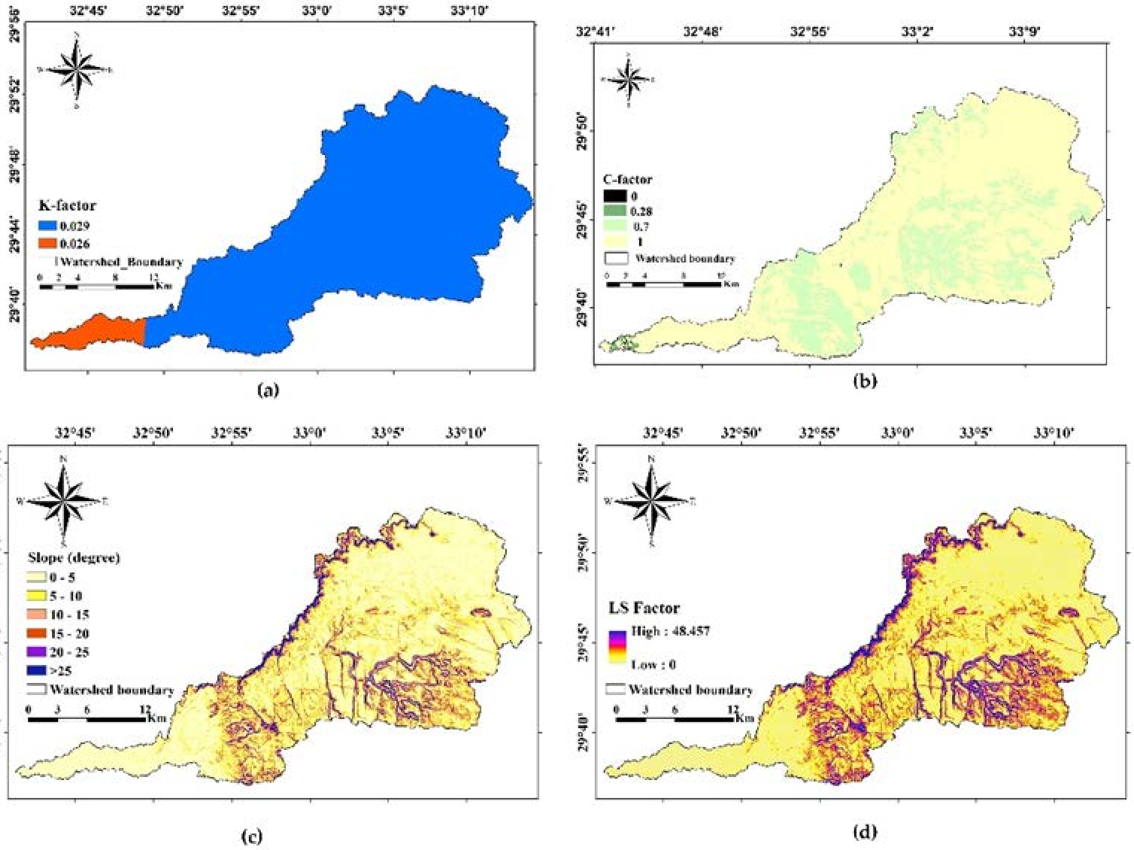

Figure 4. Distribution map of different parameters in the study area (a) K-factor, (b) C-factor, (c) Slope in degree, (d) LS factor.

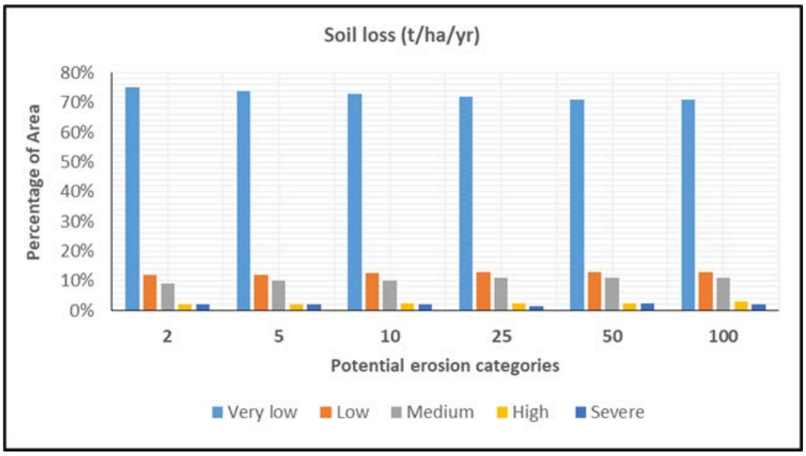

Figure 5. Potential erosion categories of Wadi Sudr watershed at different recurrence intervals.

equation of the USDA (USDA, 1979); the estimated values for SDR ranged from 0.3 to 0.43. SDR has an inverse relationship with the sub-watershed area, meaning that sub-basins with larger areas have lower SDR values, while smaller sub-basins exhibit higher SDR values (see Figure 7). The predicted sediment yield was calculated for different recurrence intervals across all Wadi Sudr sub-watersheds, with sediment yield depending on soil loss and SDR in each sub- watershed. The TR has a substantial influence on predicting sediment yield (see Figure 8). It was observed that the maximum sediment yield was found in the Al-Athamy, B4, B2, and B6 sub-watersheds. These sub-watersheds are characterized by steep slopes with bare land, a lack of conservation practices, and high soil loss, while the minimum sediment yield is represented by areas with plain slopes and agricultural lands.

3.3. Management of soil erosion and sediment yield

The Al-Athamy sub-basin has the highest values of soil erosion and sediment yield, covering an area of 124.3 km², making it the largest sub-basin. Its (LU/LC)

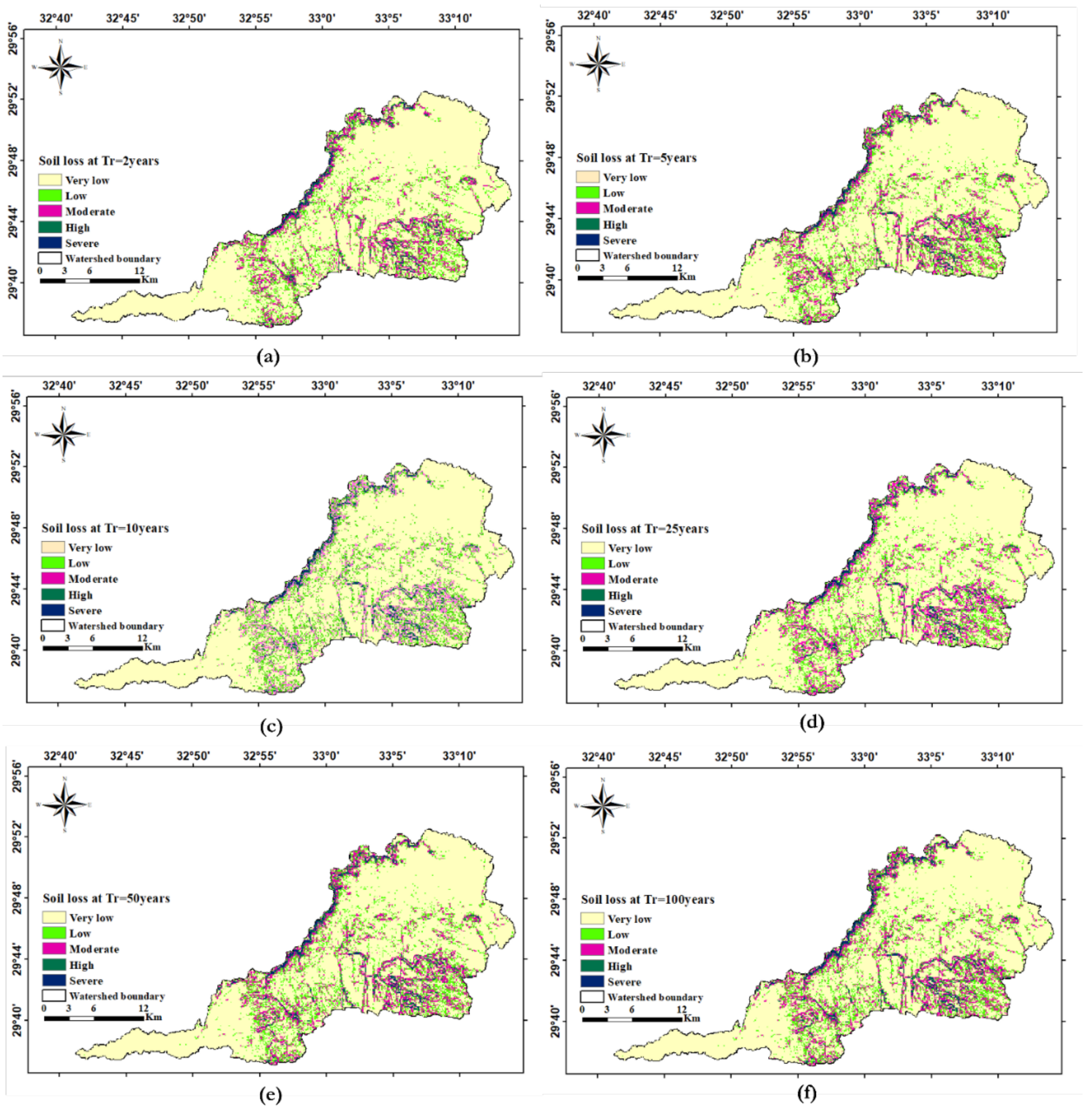

Figure 6. Soil losses at different recurrence intervals (a) TR2; (b) TR5; (c) TR10; (d) TR25; (e) TR50; (f) TR100.

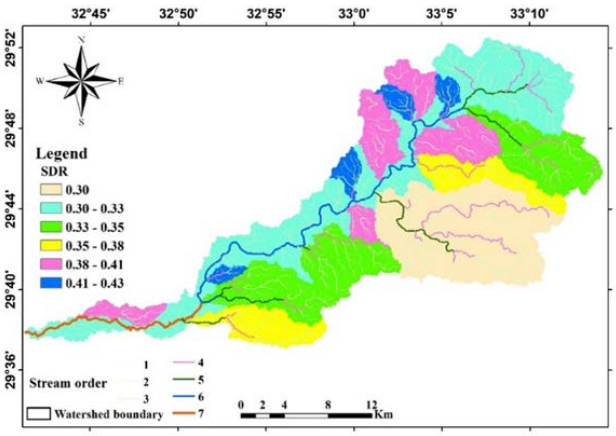

Figure 7. SDR values in all Wadi Sudr sub-watershed.

consists of bare land and rangeland, with no vegetated areas, which makes it unsuitable for vegetation-related practices. Therefore, we proposed two scenarios to protect it from soil erosion using Mulching and Check Dams.

3.3.1 Using Mulching for protecting Al-Athamy sub-basin from soil erosion

To apply the mulching scenarios, we take a new P-factor value of 0.26, as stated by (David, 1988). The mulching scenarios were implemented in Al-Athamy focusing particularly on hotspot areas along the tributaries of the streams. The buffer method was applied using ArcGIS 10.4 software. Mulching was applied in the Al-Athamy sub-basin with three scenarios. The first scenario covers 11,680 m along the stream tributaries, representing 8% of the total stream length. The second scenario covers 25,980 m, accounting for 18% of the total stream length, and the third scenario covers 32,320 m, representing 22% of the total stream length (Figure 9).

After applying the mulching scenarios, soil erosion decreased by 3%, 7% and 9%. However, sediment yield was reduced by 19%, 23%, and 24% in the three scenarios, respectively as shown in Figure 10.

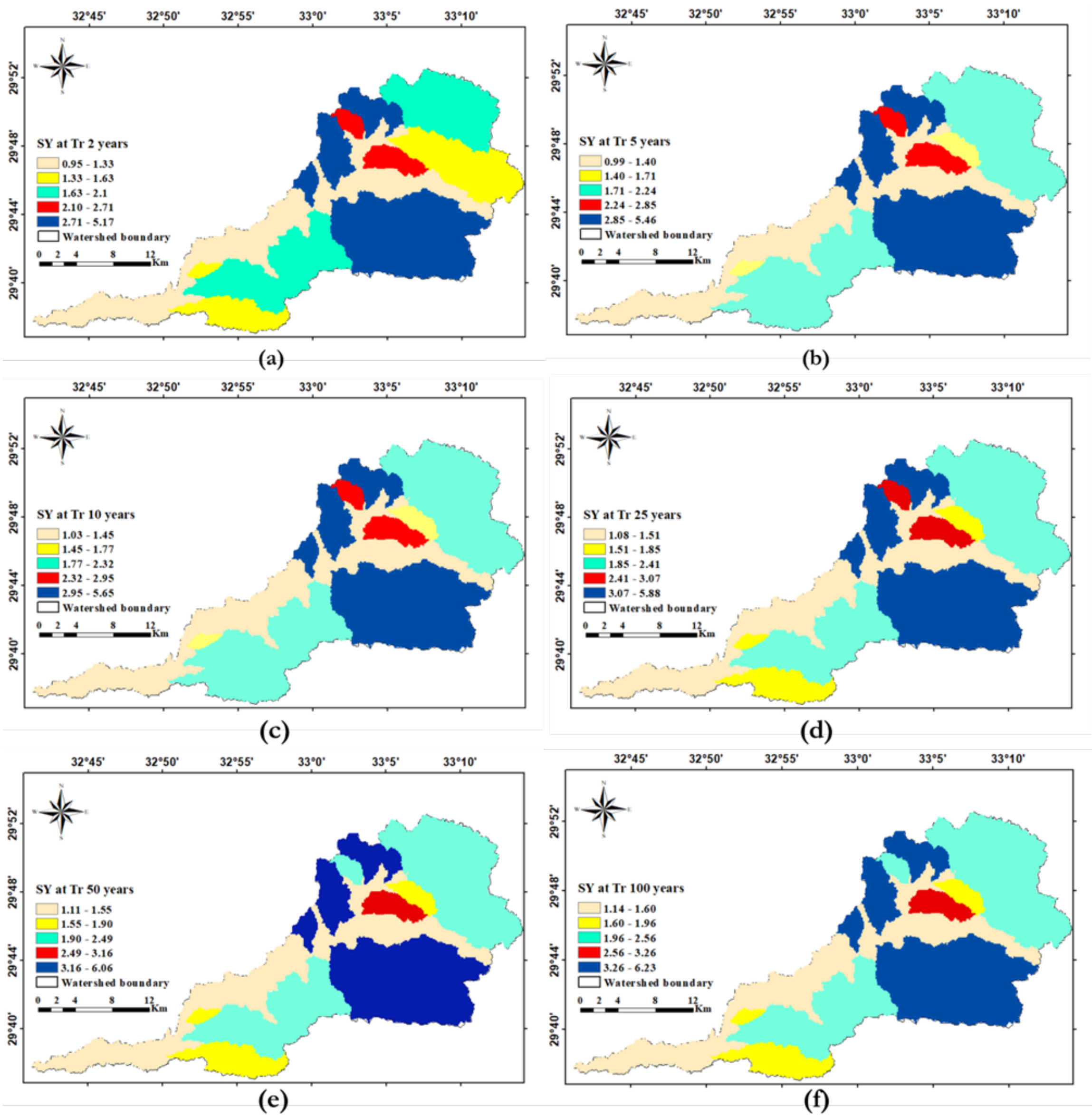

Figure 8. Sediment yield at different recurrence intervals in Wadi Sudr watershed (a)TR2; (b)TR5; (c)TR10; (d)TR25; (e)TR50; (f)TR100

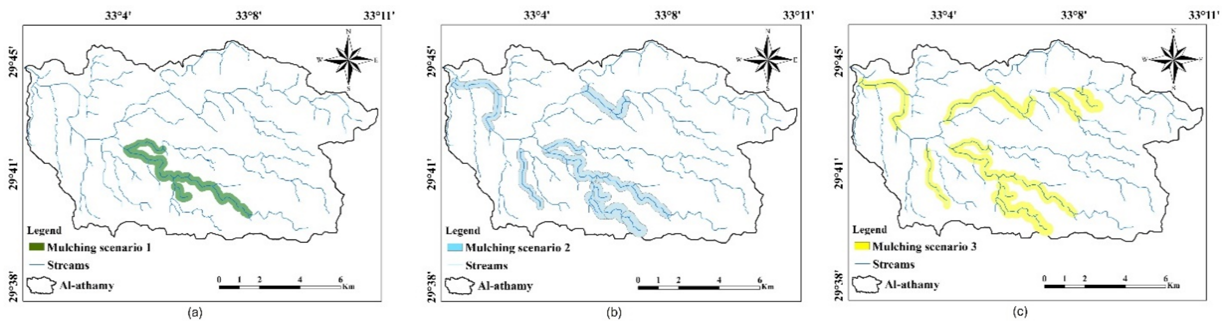

Figure 9. Mulching locations in Al-Athamy sub-basin (a) 1st scenario, (b) 2nd scenario, and (c) 3rd scenario.

The mulching scenarios are cheap and applicable in any area and give good improvement for decreasing both soil erosion and sediment yield. However, the reduction in sediment yield is quite high (19-24%) compared to soil erosion (3-9%) as shown in Figure 10.

3.3.2 Using Check Dams for protecting Al-Athamy sub-basin from soil erosion

We also implemented two check dams with varying heights, both dams' height ranging from 10 to 20 m, to assess their impact on reducing soil erosion and sediment yield. The trap efficiency of the check dam

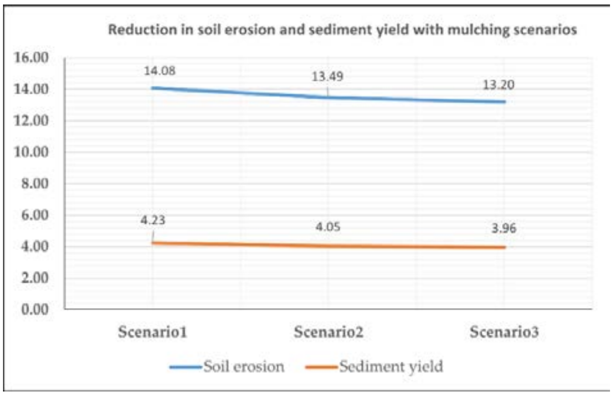

Figure 10. Mulching scenarios and their influence on soil erosion and sediment yield in Al-Athamy sub-basin.

was estimated using Eq. 11

$$TE = \frac{S_{in} - S_{out}}{S_{in}} \quad (11)$$

where,

TE represents trap efficiency.

Sin is the sediment that enters the check dam.

Sout is the dam's outflow.

In Al-athamy sub-basin, we take the value of the trapping efficiency of the check dam by 1 because the sediments from the upstream were eroded in the dam (Zhao et al., 2017).

The P-factor is estimated by Eq. 12

$$P = 1 - TE \quad (12)$$

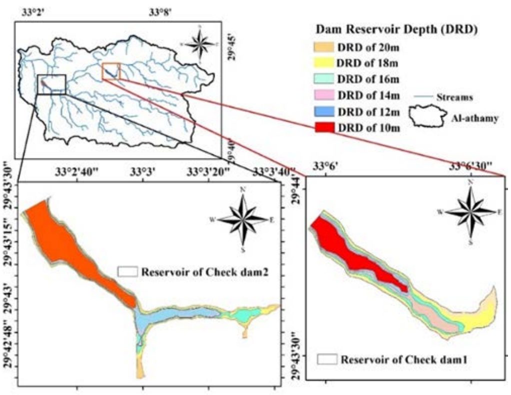

Figure 11. Locations of Check Dams in Al-Athamy sub-basin.

We considered different height variations for both dams (Figure 11). The reduction in soil erosion has decreased due to using check dam 1 by 0.04%, 0.05%, 0.07%, 0.09%, 0.11%, and 0.14%. The reduction in soil erosion when using check dam 2 was 0.14%, 0.18%, 0.20%, 0.24%, 0.27%, and 0.30% at all height variations, respectively (see Figure 12). However, the reduction in sediment yield was constant across the different heights, with a percentage reduction of 35% and 86% for check dam 1 and check dam 2, respectively.

The second check dam showed a greater reduction in sediment yield compared to the first. This is due to the second dam having a larger catchment area of104 km², whereas the first dam's catchment area was only 27 km². This indicates that as the catchment area increases and sediment yield decreases, the dam effectively traps sediments from upstream.

3.3.3. Comparison between Mulching scenarios and Check dam scenarios

The comparison between different management scenarios to reduce the soil erosion using three mulching scenarios and two check dams; check dam 1 and check dam 2 as is shown in Figure 13. Mulching has a moderate effect on reducing soil erosion, with reduction percentages ranging from 3% to 9% across the three mulching scenarios. The impact of mulching on sediment yield is more significant, with reductions increasing from 19% in the 1st mulching scenario to 24% in the 3rd mulching scenario. This indicates that mulching becomes more effective in controlling soil erosion. Both check dams show a negligible reduction in soil erosion. However, they have a substantial impact on sediment yield reduction, particularly check dam 2, which reduces sediment yield by 86%. Check dam 1 also shows a significant reduction of around 35%. This indicates that check dams play a significant role in controlling sediment yield, although they are less effective in reducing soil erosion. Compared to the check dam scenarios, the mulching scenarios result in a greater reduction in soil erosion. However, the mulching scenarios show a smaller reduction in sediment yield compared to the check dam scenarios.

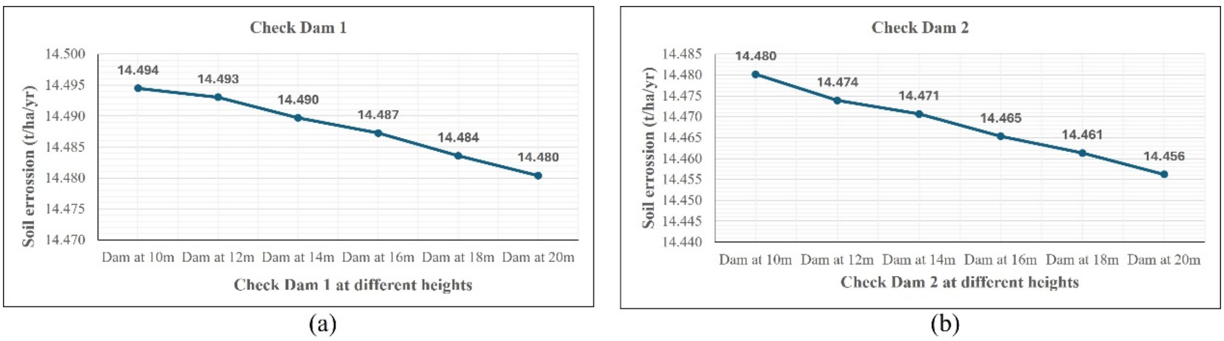

Figure 12. The effect of check dams in Al-Athamy sub-basin in reducing soil erosion, (a) check dam1, (b) check dam2.

This is because check dams are the most effective management practice for reducing sediment yield, as they trap sediments from upstream of the dam.

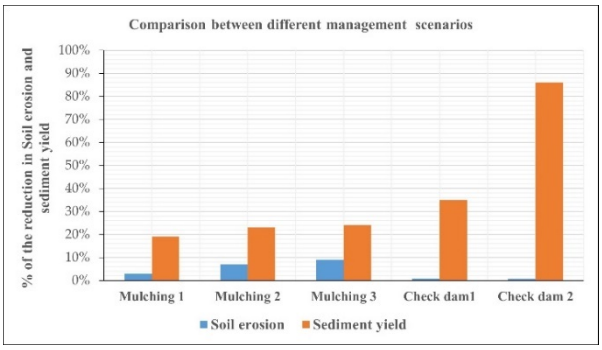

Figure 13. Comparison of the reduction percentages of soil erosion and sediment yield after applying mulching and check dam scenarios.

3.4. Forecasting the reduction in soil erosion and sediment yield

Two empirical equations are developed for forecasting the reduction percentages of soil erosion and sediment yield based on the mulching technique. The equations were developed by correlating several parameters such as sub-basin area (A), mulch length (L), mulch area (Ar), and the ratio of mulch length to total stream length (Lr) using multiple regression analysis in Excel. These equations were used to forecast the soil erosion reduction percentage (Re) and sediment yield reduction percentage (Rs), as shown in Equations 13 and 14. The reduction percentage due to mulching is expressed as follows:

$$Re = 0.305 \times Lr + 1.1 \times 10^{-6} L - 0.00765 \quad (13)$$

$$Rs = 4.26 \times 10^{-6} L + 0.1 \quad (14)$$

Where Re is the reduction percentage in soil erosion based on mulch, Rs represents the reduction percentage in sediment yield after applying much, L is the mulch length (m), and Lr is the relative mulch length to the total stream length.

The correlation coefficient and the standard error for Equations 13 and 14 are 94% and 0.035, respectively. Figures 14a and 14c represent the predicted reduction percentages versus residuals, with a red dashed line indicating zero residuals; the residuals differ for each predicted value. Figures 14b and 14d compare the predicted reduction percentages using Equations 13 and 14 with the measured reduction percentages, where the two data sets are plotted against each other, showing their close alignment. All these figures indicate how well Equations 13 and 14 fit the data and, therefore, could be used to forecast the reduction percentage in sediment yield and soil erosion based on mulching technique around streamlines in any study area with similar characteristics. These equations will aid policymakers in evaluating mulching's impact on sediment yield and soil erosion.

In this study, the soil erosion and sediment yield were estimated and predicted at various recurrence intervals to achieve the aim of the research. Additionally, management practices were proposed to control soil erosion and sediment yield in hotspot areas, particularly in the Al-Athamy sub-basin. The study also developed empirical equations for forecasting the reduction percentages of soil erosion and sediment yield using a regression analysis model, which could help to predict the impact of mulching in the study area and other semi-arid watersheds.

Several studies indicate the effectiveness of these management practices. Bombino et al. (Bombino et al., 2021) found a 75-80% reduction in soil erosion after applying mulching with pruning residues. Check dams are also an efficient sediment yield management practice, reducing sediment yield by 51.9% (Zhao et al., 2017). This study examined the two methods to protect the current study area from soil erosion and sediment yield to assist policymakers in implementing appropriate management scenarios for conserving lives and infrastructure in these vital areas.

According to soil erosion results our study aligns directly with (Sandeep et al., 2021), who stated that 86% of their study area was classified as low potential erosion risk (0-10 tons/ha/year). In contrast, our results show a slightly broader range, including erosion rates up to 11.2 t/ha/year, which may account for a slightly higher percentage in the low and very low categories. Additionally, our findings are higher than (Balasubramani et al., 2015), who reported that 76% of a semi-arid watershed was classified as low potential erosion risk (0-10 tons/ha/year).

Furthermore, we observe a much higher percentage of low erosion risk compared to (Sathiyamurthi et al., 2023), who reported that in 2009, only 35% of the area was classified under low erosion risk, which is considerably lower than the 86% in our study. Additionally, our study shows a significantly higher percentage of land under low erosion risk compared to (Djoukbala et al., 2018), who found that 54.3% of semi-arid regions were classified under the low erosion risk category (0-4 t/ha/year).

4. CONCLUSIONS

The SDR and RUSLE models were integrated to estimate and predict soil erosion and sediment yield based on rainfall events at different recurrence intervals. Then management scenarios were proposed to protect the hotspot areas using mulching and check dams in, and the reduction percentages in soil erosion and sediment

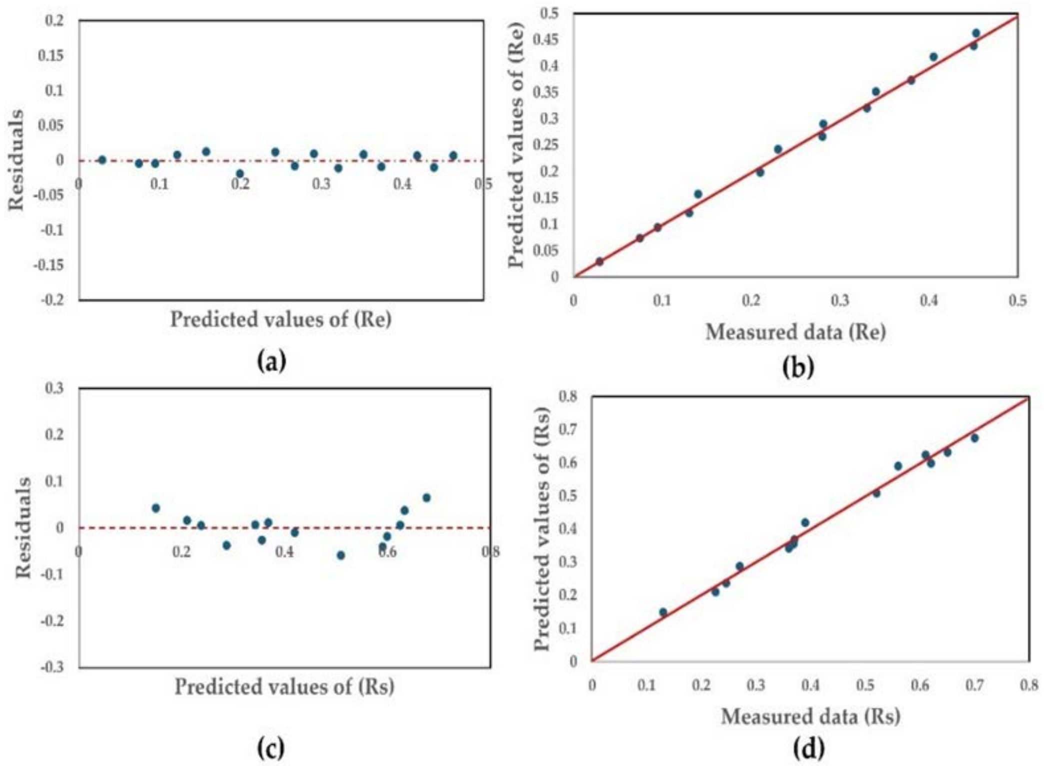

Figure 14. (a) predicted Re versus Residuals, (b) Measured Re versus values predicted from Equation 13, (c) the predicted sediment yield reduction versus The Residuals, and (d) Measured Rs versus Predicted values from equation 14.

yield were forecasted based on the implementation of the mulching technique using the multi-regression analysis. There are no prior studies on soil erosion and sediment yield management in Wadi Sudr. Therefore, this research fills that gap, helping policymakers implement appropriate management practices to control soil erosion and sediment yield while conserving soil, protecting infrastructure, and reducing land degradation. A reduction in soil erosion of 3%, 7%, and 9% was found after applying 11,680 m, 25,980 m, and 32,320 m mulch length, respectively. Meanwhile, sediment yield was reduced by 19%, 23%, and 24% with the 1st, 2nd, and 3rd mulching scenarios, respectively. Both check dams showed minimal reduction in soil erosion at all heights. However, check dam 1 reduced sediment yield by 35% at all depths, while check dam 2 resulted in a drastic and constant reduction of 86% in sediment yield at all heights.

The key findings of this study conducted as follows:

1) Recurrence intervals are highly significant in forecasting soil loss and sediment yield.

2) The most dominant factors in soil erosion estimation are LS and C-factor.

3) Soil erosion and sediment yield highest values are found in mountainous and steeply sloped areas with areas with no management practices.

4) Check dams are effective in sediment yield reduction. However, check dams have limitations, such as being more expensive and having a shorter lifespan due to sediment accumulation.

5) Mulching is an effective management scenario, as it significantly reduces soil erosion and sediment yield. In addition, it is a cost-effective and long-lasting management practice.

6) Forecasting the percentage reduction in soil erosion and sediment yield is crucial for aiding policymakers in conserving soil and water and managing semi-arid areas.

It is recommended that future studies include climate change scenarios in models to evaluate the potential impacts of more intense or frequent rainfall events on soil erosion and sediment yield. To ensure the reliability and applicability of the empirical equations, they should be tested across various watersheds with different characteristics. Additionally, a cost-benefit analysis comparing mulching and check dams, considering long-term maintenance and material costs, should be conducted. Future research should also apply land use change scenarios and integrate RUSLE/SDR models with machine learning.

REFERENCES

Abbasi, N. A., Xu, X., Lucas-Borja, M. E., Dang, W., & Liu, B., 2019. *The use of check dams in watershed management projects: Examples from around the world*. Sci Total Environ, 676, 683-691.

Abd-Elaty, I., Shoshah, H., Zeleňáková, M., Kushwaha, N. L. & El-Dean, O. W., 2022. *Forecasting of Flash Floods Peak Flow for Environmental Hazards and Water Harvesting in Desert Area of El-Qaa Plain, Sinai*. International Journal of Environmental Research and Public Health, 19**,** 6049.

Abebe, N., Eekhout, J., Vermeulen, B., Boix-Fayos, C., De Vente, J., Grum, B., Hoitink, T., & Baartman, J., 2023. *The potential and challenges of the 'RUSLE-IC-SDR' approach to identify sediment dynamics in a Mediterranean catchment*. Catena, 233**,** 107480.

Adekalu, K. O., Olorunfemi, I. A., & Osunbitan, J. A., 2007. *Grass mulching effect on infiltration, surface runoff and soil loss of three agricultural soils in Nigeria*. Bioresour Technol, 98**,** 912-7.

Al-Bassam, A. M., Zaidi, F. K., & Hussein, M. T., 2014. *Natural hazards in Saudi Arabia*. Extreme natural events, disaster risks and societal implications**,** 243-251.

Alhamid, A. A., & Reid, I., 2002. *Sediment and the vulnerability of water resources*. Hydrology of Wadi Systems, IHP Network on Wadi Hydrology in the Arab region, 55**,** 37-55.

Ali, A. M., 2023. *Assessing flood risks in arid zones by linking remote sensing techniques and GIS*. Journal of Al-Azhar University Engineering Sector, 18**,** 850-868.

Arnold, J. G., & Fohrer, N., 2005. *SWAT2000: current capabilities and research opportunities in applied watershed modelling*. Hydrological Processes: An International Journal, 19**,** 563-572.

Aslam, B., Khalil, U., Saleem, M., Maqsoom, A., & Khan, E., 2021. *Effect of multiple climate change scenarios and predicted land-cover on soil erosion: a way forward for the better land management*. Environ Monit Assess, 193**,** 754.

Assis, K. G. O., Da Silva, Y., Lopes, J. W. B., Medeiros, J. C., Teixeira, M. P. R., Rima, F. B., & Singh, V. P., 2021. *Soil loss and sediment yield in a perennial catchment in southwest Piaui, Brazil*. Environ Monit Assess, 193**,** 26.

Beasley, D. B., Huggins, L. F., & Monke, E. J., 1980. *ANSWERS: a model for watershed planning*. Transactions, American Society of Agricultural Engineers, 23**,** 938-944.

Boix-Fayos, C., De Vente, J., Martínez-Mena, M., Barberá, G. G., & Castillo, V., 2008. *The impact of land use change and check-dams on catchment sediment yield*. Hydrological Processes, 22**,** 4922-4935.

Bombino, G., Denisi, P., Gómez, J. A., & Zema, D. A., 2021. *Mulching as best management practice to reduce surface runoff and erosion in steep clayey olive groves*. International Soil and Water Conservation Research, 9**,** 26-36.

Choudhury, M., & Nayak, T., 2003. *Estimation of soil erosion in Sagar Lake catchment of Central India*. Proceedings of the international conference on water and environment, 387-392.

Conoco, 1987. *Geological Maps of Egypt Scale 1:500,000. Sheet Nos. NG 36 NW Cairo*. The Egyptian General Petroleum Corporation, Egypt.

Darwish, K. M., Abdel Kawy, W. A. M., Afifi, A. A., & Zölitz, R., 2015. *Estimating the rainfall erosivity for management planning in the Eastern Desert, Egypt*. Geocarto International, 31**,** 1123-1141.

David, W. P., 1988. *Soil and water conservation planning: policy issues and recommendations*. Philippine Institute for Development Studies.

De Jong, S., Paracchini, M., Bertolo, F., Folving, S., Megier, J., & De Roo, A., 1999. *Regional assessment of soil erosion using the distributed model SEMMED and remotely sensed data*. Catena, 37**,** 291-308.

Dong, H., Song, Y., Chen, L., Liu, H., Fu, X., & Xie, M., 2022. *Soil erosion and human activities over the last 60 years revealed by magnetism, particle size and minerals of check dams sediments on the Chinese Loess Plateau*. Environmental Earth Sciences, 81.

El Jazouli, A., Barakat, A., Ghafiri, A., El Moutaki, S., Ettaqy, A., & Khellouk, R., 2017. *Soil erosion modeled with USLE, GIS, and remote sensing: a case study of Ikkour watershed in Middle Atlas (Morocco)*. Geoscience Letters, 4.

Elewa, H. H., Nosair, A. M., & Ramadan, E. M., 2020. *Determination of Potential Sites and Methods for Water Harvesting in Sinai Peninsula by the Application of RS, GIS, and WMS Techniques*. *In:* NEGM, A. M. (ed.) Flash Floods in Egypt. Cham: Springer International Publishing.

Erencin, Z., Shresta, D., & Krol, I. B., 2000. *C-factor mapping using remote sensing and GIS*. Case study Lom SakLom Kao Thail Geogr Inst Justus-Liebig-Univ Giess Intern Inst Aerosp Surv Earth SciITC Enschede Netherland.

Fao,1990. *Conservation des ressources naturelles en zones arides.* Cahier FAO: Conserv Des Sols 50:62.

Fathy, I., Negm, A. M., El-Fiky, M., Nassar, M., & Al-Sayed, E., 2015. *Runoff hydrograph modeling for arid regions: case study—Wadi Sudr-Sinai*. Int Water Technol J IWTJ, 5**,** 58-68.

Gabr, S., & El Bastawesy, M., 2015. *Estimating the flash flood quantitative parameters affecting the oil-fields infrastructures in Ras Sudr, Sinai, Egypt, during the January 2010 event*. The Egyptian Journal of Remote Sensing and Space Science, 18**,** 137-149.

Gashaw, T., Dile, Y. T., Worqlul, A. W., Bantider, A., Zeleke, G., Bewket, W., & Alamirew, T., 2021. *Evaluating the Effectiveness of Best Management Practices On Soil Erosion Reduction Using the SWAT Model: for the Case of Gumara Watershed, Abbay (Upper Blue Nile) Basin*. Environ Manage, 68**,** 240-261.

Gelagay, H. S., & Minale, A. S., 2016. *Soil loss estimation using GIS and Remote sensing techniques: A case of Koga watershed, Northwestern Ethiopia*. International Soil and Water Conservation Research, 4**,** 126-136.

Hasanein, A., 1989. *Geology of water resources in Wadi Sudr-Wadi Gharandal area, Gulf of Suez region, Sinai Peninsula, Egypt.* M. Sc. Thesis, Faculty of Science, Ain Shams University, Egypt.

Kawy, W. A. A., & El-Nady, M. A., 2012. *Erosion Assessment Using Revised Universal Soil Loss Equation for Selective Dry Valleys In the Eastern Desert of Egypt*.

Khairunnisa, F., Tambunan, M. P., & Marko, K., 2020. *Estimation of soil erosion by USLE model using GIS technique (A case study of upper Citarum Watershed)*. IOP Conference Series: Earth and Environmental Science, 561**,** 012038.

Kumarasinghe, U., 2021. *A review on new technologies in soil erosion management*. J. Res. Technol. Eng, 2**,** 120-127.

Leta, M. K., Waseem, M., Rehman, K., & Tranckner, J., 2023. *Sediment yield estimation and evaluating the best management practices in Nashe watershed, Blue Nile Basin, Ethiopia*. Environ Monit Assess, 195**,** 716.

Maqsoom, A., Aslam, B., Hassan, U., Kazmi, Z. A., Sodangi, M., Tufail, R. F., & Farooq, D., 2020. *Geospatial assessment of soil erosion intensity and sediment yield using the Revised Universal Soil Loss Equation (RUSLE) model*. ISPRS International Journal of Geo-Information, 9**,** 356.

Mhaske, S. N., Pathak, K., Dash, S. S., & Nayak, D. B., 2021. *Assessment and management of soil erosion in the hilltop mining dominated catchment using GIS integrated RUSLE model*. J Environ Manage, 294**,** 112987.

Millward, A. A. & Mersey, J. E., 1999. *Adapting the RUSLE to model soil erosion potential in a mountainous tropical watershed*. CATENA, 38**,** 109-129.

Morgan, R., Quinton, J., Smith, R., Govers, G., Poesen, J., Auerswald, K., Chisci, G., Torri, D. & Styczen, M., 1998. *The European Soil Erosion Model (EUROSEM): a dynamic approach for predicting sediment transport from fields and small catchments*. Earth Surface Processes and Landforms: The Journal of the British Geomorphological Group, 23**,** 527-544.

Nearing, M. A., Foster, G. R., Lane, L.J., & C. Finkner, S., 1989. *A Process-Based Soil Erosion Model for USDA-Water Erosion Prediction Project Technology*. Transactions of the ASAE, 32**,** 1587-1593, https://doi.org/10.13031/2013.31195

Pancholi, V., Lodha, P. & Prakash, I., 2015. *Estimation of soil erosion for Vishwamitri River Watershed using universal soil loss equation and GIS*. International Journal for Scientific Research & Development, 3**,** 444-449.

Pham, T. G., Degener, J., & Kappas, M., 2018. *Integrated universal soil loss equation (USLE) and Geographical Information System (GIS) for soil erosion estimation in A Sap basin: Central Vietnam*. International Soil and Water Conservation Research, 6**,** 99-110.

Phinzi, K., & Ngetar, N. S., 2019. *The assessment of water-borne erosion at catchment level using GIS-based RUSLE and remote sensing: A review*. International Soil and Water Conservation Research, 7**,** 27-46.

Pimentel, D., 2006. *Soil Erosion: A Food and Environmental Threat*. Environment, Development and Sustainability, 8**,** 119-137.

Rajbanshi, J., & Bhattacharya, S., 2020. *Assessment of soil erosion, sediment yield and basin specific controlling factors using RUSLE-SDR and PLSR approach in Konar river basin, India*. Journal of Hydrology, 587**,** 124935.

Ramadan, E. M., Shahin, H. A., Abd-Elhamid, H. F., Zelenakova, M., & Eldeeb, H. M., 2022. *Evaluation and Mitigation of Flash Flood Risks in Arid Regions: A Case Study of Wadi Sudr in Egypt*. Water, 14**,** 2945.

Renard, K. G. 1997. *Predicting soil erosion by water: a guide to conservation planning with the Revised Universal Soil Loss Equation (RUSLE)*. United States Government Printing.

Renard, K. G., Foster, G. R., Weesies, G. A., Mccool, D. K. & Yoder, D. C. *Predicting soil erosion by water : a guide to conservation planning with the Revised Universal Soil Loss Equation (RUSLE)*. 1997.

Salhi, A., El Hasnaoui, Y., Perez Cutillas, P., & Heggy, E., 2023. *Soil erosion and hydroclimatic hazards in major African port cities: the case study of Tangier*. Sci Rep, 13**,** 13158.

Saoud, M., & Meddi, M., 2023. *Estimation of soil erosion and sediment yield in Wadi El Hachem watershed (Algeria) using the RUSLE-SDR approach*. Journal of Mountain Science, 20**,** 367-380.

Selmy, S. A. H., Al-Aziz, S. H. A., Jiménez-Ballesta, R., García-Navarro, F. J., & Fadl, M. E., 2021. *Modeling and assessing potential soil erosion hazards using usle and wind erosion models in integration with gis techniques: Dakhla oasis, egypt*. Agriculture, 11**,** 1124.

Shi, P., Zhang, Y., Ren, Z., Yu, Y., Li, P., & Gong, J., 2019. *Land-use changes and check dams reducing runoff and sediment yield on the Loess Plateau of China*. Sci Total Environ, 664**,** 984-994.

Silva, R., Santos, C. A. G., & Montenegro, S., 2013. *Identification of critical erosion prone areas and estimation of natural potential for erosion using GIS and Remote Sensing*. Revista Brasileira de Cartografia, 65**,** 125-136.

Soliman, M. M., Hegab, I. A., & El-Sayied, S. S., 2017. *Geomorphological, pedological studies and evaluation of some soils in Wadi Sudr, Sinai Peninsula, Egypt*. Menoufia J. Soil Sci.,, 2**,** 293-307.

Thomas, J., Joseph, S., & Thrivikramji, K. P., 2018. *Assessment of soil erosion in a monsoon-dominated mountain river basin in India using RUSLE-SDR and AHP*. Hydrological Sciences Journal, 63**,** 542-560.

Usda, S., 1972. *National engineering handbook, section 4: Hydrology*. Washington, DC.

Usda, S., 1979. *United States Department of Agriculture-Soil Conservation Service*. National Engineering Handbook, Sec, 4.

Venter, Z. S., Barton, D. N., Chakraborty, T., Simensen, T., & Singh, G., 2022. *Global 10 m Land Use Land Cover Datasets: A Comparison of Dynamic World, World Cover and Esri Land Cover*. Remote Sensing, 14**,** 4101.

Williams, J., 1975. *Sediment routing for agricultural watersheds 1*. JAWRA Journal of the American Water Resources Association, 11**,** 965-974.

Wischmeier, W. H., & Smith, D. D., 1978a. *Predicting rainfall erosion losses: a guide to conservation planning*, Department of Agriculture, Science and Education Administration.

Wischmeier, W. H., & Smith, D. D., 1978b. *Predicting Rainfall Erosion Losses: A Guide to Conservation Planning, Science, US Department of Agriculture Handbook,*, Department of Agriculture, Science and Education Administration.

Zerihun, M., Mohammedyasin, M. S., Demeke, S., Adem, A. A., & Lakew, M., 2018. *Assessment of soil erosion using RUSLE, GIS and remote sensing in NW Ethiopia*. Geoderma Regional, 12**,** 83-90.

Zhao, G., Kondolf, G. M., Mu, X., Han, M., He, Z., Rubin, Z., Wang, F., Gao, P., & Sun, W., 2017. *Sediment yield reduction associated with land use changes and check dams in a catchment of the Loess Plateau, China*. Catena, 148**,** 126-137.

Received: 21 .01. 2025
Revised: 16. 04. 2025
Accepted: 19. 04. 2025
Published: 22. 04. 2025